A Combined Theoretical and Experimental Study of the Reaction Products of Laser-Ablated Thorium Atoms with CO: First Identification of the CThO, $CThO^-$, OThCCO, OTh(η^3-CCO), and $Th(CO)_n$ ($n = 1-6$) Molecules

Jun Li and Bruce E. Bursten*

Department of Chemistry, The Ohio State University, Columbus, Ohio 43210

Mingfei Zhou and Lester Andrews*

Department of Chemistry, University of Virginia, Charlottesville, Virginia 22904-4319

Received July 16, 2001

Laser-ablated thorium atoms have been reacted with CO molecules during condensation in excess neon. Absorptions at 617.7 and 812.2 cm^{-1} are assigned to Th−C and Th−O stretching vibrations of the CThO molecule. Absorptions at 2048.6, 1353.6, and 822.5 cm^{-1} are assigned to the OThCCO molecule, which is formed by CO addition to CThO and photochemical rearrangement of $Th(CO)_2$. The OThCCO molecule undergoes further photoinduced rearrangement to OTh(η^3-CCO), which is characterized by C−C, C−O, and Th−O stretching vibrations at 1810.8, 1139.2, and 831.6 cm^{-1}. The $Th(CO)_n$ ($n = 1-6$) complexes are formed on deposition or on annealing. Evidence is also presented for the $CThO^-$ and $Th(CO)_2^-$ anions, which are formed by electron capture of neutral molecules. Relativistic density functional theory (DFT) calculations of the geometry structures, vibrational frequencies, and infrared intensities strongly support the experimental assignments. It is found that CThO is an unprecedented actinide-containing carbene molecule with a triplet ground state and an unusual bent structure ($\angle$CThO = 109°). The OThCCO molecule has a bent structure while its rearranged product OTh(η^3-CCO) is found to have a unique exocyclic structure with side-bonded CCO group. We also find that both $Th(CO)_2$ and $Th(CO)_2^-$ are, surprisingly, highly bent, with the $\angle$C−Th−C bond angle being close to 50°; the unusual geometries are the result of extremely strong Th-to-CO back-bonding, which causes significant three-centered bonding among the Th atom and the two C atoms.

Introduction

Carbon monoxide activation and reduction are important in great many of industrial processes such as hydroformylation, alcohol synthesis, and acetic acid synthesis.[1] While CO activation has traditionally been accomplished mainly via transition-metal complexes, actinide complexes have been found to possess fascinating bonding modes in activating CO,[2−4] NO,[5] and even N_2 molecules.[6,7] We have investigated the reaction of laser-ablated thorium atoms with N_2 and found that the dinitrogen bonds can be significantly weakened by actinide complexation.[8] Inasmuch as CO is isoelectronic to N_2, it is therefore interesting to explore how the CO molecules react with actinides such as thorium.

Contrary to the extensive investigations of transition metal carbonyl complexes, actinide carbonyl complexes have been largely unknown for a long time. The coordination chemistry of CO with actinide elements is a relatively new and unexplored area, in part because of the experimental challenges faced in handling and characterizing the actinide compounds. Recently several actinide monocarbonyl complexes have been experimentally characterized,[9−11] and theoretical studies of the electronic structures and bonding of these unique compounds have been carried out.[12,13] Even though an earlier thermal uranium atom matrix isolation investigation has tentatively identified uranium carbonyls in solid argon,[14] little is known so far about the reactions between actinide metal atoms and CO molecules. Very recently, we have used infrared spectroscopy and density functional theoretical studies to characterize the products of the reaction of laser-ablated uranium atoms with

(1) See, for example: (a) Collman, J. P.; Hegedus, L. S. *Principles and Applications of Organotransition Metal Chemistry*; University Science Books: Mill Valley, CA, 1980. (b) Muetterties, E. L.; Stein, J. *Chem. Rev.* **1979**, *79*, 479.
(2) Moloy, K. G.; Marks, T. J. *J. Am. Chem. Soc.* **1984**, *106*, 7051.
(3) Tatsumi, K.; Nakamura, A.; Hofmann, P.; Stauffert, P.; Hoffmann, R. *J. Am. Chem. Soc.* **1985**, *107*, 4440.
(4) Sonnenberger, D. C.; Mintz, E. A.; Marks, T. J. *J. Am. Chem. Soc.* **1984**, *106*, 3484.
(5) Zhou, M. F.; Andrews, L. *J. Chem. Phys.* **1999**, *110*, 10370.
(6) (a) Roussel, P.; Scott, P. *J. Am. Chem. Soc.* **1998**, *120*, 1070. (b) Roussel, P.; Tinker, N. D.; Scott, P. *J. Alloys Compd.* **1998**, *271−273*, 150.
(7) Odom, A. L.; Arnold, P. L.; Cummins, C. C. *J. Am. Chem. Soc.* **1998**, *120*, 5836.
(8) Kushto, G. P.; Souter, P. F.; Andrews, L. *J. Chem. Phys.* **1998**, *108*, 7121.
(9) Brennan, J. G.; Andersen, R. A.; Robbins, J. L. *J. Am. Chem. Soc.* **1986**, *108*, 335.
(10) Parry, J.; Carmona, E.; Coles, S.; Hursthouse, M. *J. Am. Chem. Soc.* **1995**, *117*, 2649.
(11) del Mar Conejo, M.; Parry, J. S.; Carmona, E.; Schultz, M.; Brennann, J. G.; Beshouri, S. M.; Andersen, R. A.; Rogers, R. D.; Coles, S.; Hursthouse, M. B. *Chem. Eur. J.* **1999**, *5*, 3000.
(12) Tatsumi, K.; Hoffmann, R. *Inorg. Chem.* **1984**, *23*, 1633.
(13) (a) Bursten, B. E.; Strittmatter, R. J. *J. Am. Chem. Soc.* **1987**, *109*, 6606. (b) Bursten, B. E.; Strittmatter, R. J. *Angew. Chem., Int. Ed. Engl.* **1991**, *30*, 1069.
(14) Slater, J. L.; Sheline, R. K.; Lin, K. C.; Weltner, W., Jr. *J. Chem. Phys.* **1971**, *55*, 5129.

10.1021/ic010755m CCC: $20.00
Published on Web 09/11/2001

carbon monoxide, including a series of uranium carbonyls, the CO-insertion product CUO, and the isomeric products of the photoinduced rearrangement of uranium dicarbonyl, namely OUCCO and $(\eta^2\text{-}C_2)UO_2$.[15]

In this paper, we report a combined experimental and theoretical study of the products of the reactions of laser-ablated thorium atoms with CO in frozen neon. It is of great interest to compare the differences between thorium and uranium chemistry because Th has a transition-metal-like electron configuration ($6d^27s^2$) with two fewer valence electrons than uranium. Although the reactivity of Th with CO might be expected to parallel that of U with CO, the results presented here indicate distinct differences because of the intrinsic difference between the valence electronic structures of Th and U. This work represents the first experimental and theoretical investigation of the unique actinide metallocarbene CThO and of the first thorium carbonyl complexes.[16]

Experimental and Computational Methods

The experiment for laser ablation and matrix isolation spectroscopy has been described in detail previously.[17,18] Briefly, the Nd:YAG laser fundamental (1064 nm, 10 Hz repetition rate with 10 ns pulse width) was focused on the rotating thorium metal target (Oak Ridge National Laboratory) using low energy (1−5 mJ/pulse). Laser-ablated metal atoms were co-deposited with carbon monoxide (0.05 to 0.2%) in excess neon onto a 4 K CsI cryogenic window at 2−4 mmol/hour for 30 min to 1 h. Carbon monoxide (Matheson) and isotopic $^{13}C^{16}O$ and $^{12}C^{18}O$ (Cambridge Isotopic Laboratories) and selected mixtures were used in different experiments. Infrared spectra were recorded at 0.5 cm^{-1} resolution on a Nicolet 750 spectrometer with 0.1 cm^{-1} accuracy using a HgCdTe detector. Matrix samples were annealed at different temperatures, and selected samples were subjected to broadband photolysis by a medium-pressure mercury arc (Philips, 175W, globe removed, 240−580 nm).

The theoretical calculations were performed by using the Amsterdam Density Functional (ADF 2.3) code.[19] The generalized-gradient density functional method was employed, using the local density approach[20] with gradient-corrected Perdew-Wang 91 (PW91) exchange-correlation functionals.[21] Uncontracted triple-ζ STO basis sets were used for Th, C, and O, with d- and f-type polarization functions for C and O. Scalar relativistic (mass-velocity and Darwin) effects were taken into account by using the quasi-relativistic method,[22] and the effects of spin−orbit coupling for closed-shell molecules were evaluated by using Pauli perturbation formalism and double-group symmetry.[23] All the geometric structures were fully optimized under the proper symmetry point group via analytical energy gradient techniques. The frequency calculations were performed at the geometries optimized with only scalar relativistic effects included, because from our experience the effects of spin−orbit coupling do not significantly affect vibrational frequencies of actinide complexes.[24] Two-side displacements were employed in the numerical determination of the force-constant matrices, which partially corrects for the odd-order anharmonicity of the potential energy surface. The atomic masses used in the frequency calculations for the isotopic substitution are 232.038049 for ^{232}Th, 12.00000 and 13.00335 for ^{12}C and ^{13}C, and 15.994914 and 17.9992 for ^{16}O and ^{18}O, respectively.[25] Since potential energy surfaces of many of the species identified in this work are rather complicated, a linear transit (LT) approach with full optimization of the geometries at each step was applied in order to make sure the correct ground states and geometries corresponding to the global minimum. In calculating singlet−triplet splitting energies, the diagonal sum rule of Ziegler, Rauk, and Baerends has been applied when necessary.[26] Very tight numerical integration accuracy of INTEGRATION = 10.0 was used throughout, with the convergence thresholds set at 10^{-4} Hartree/Å for Cartesian gradients during geometry optimizations and as 10^{-8} for energy iterations during self-consistent field calculations. Further computational details were similar to those described previously.[27]

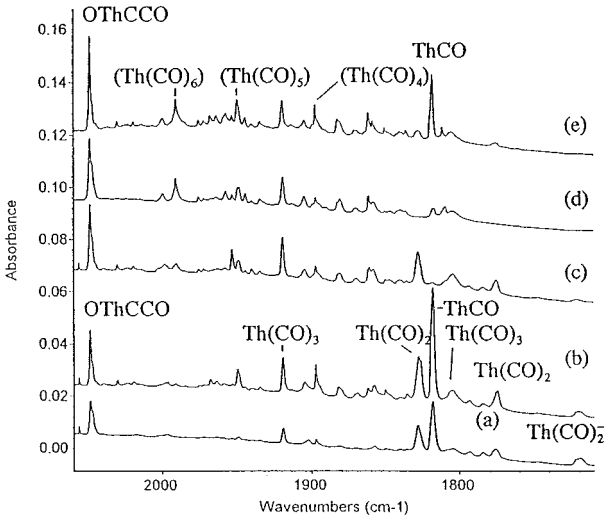

Figure 1. Infrared spectra in the 2060−1710 cm^{-1} region for laser-ablated thorium co-deposited with 0.1% CO in neon at 4K: (a) after 30 min sample deposition, (b) after annealing to 8K, (c) after 15 min $\lambda > 470$ nm photolysis, (d) after 15 min full arc photolysis, and (e) after annealing to 10K.

Experimental Results

Infrared spectra for the reaction of laser-ablated thorium with CO in excess neon reveal the strong CO absorption at 2140.7 cm^{-1}, a weak band for CO^+ at 2194.3 cm^{-1} (not shown), $(CO)_2^+$ at 2056.3 cm^{-1}, and $(CO)_2^-$ at 1517.4 cm^{-1} (not shown),[28,5] together with new product absorptions. The infrared spectra in the 2060−1710 cm^{-1} and 1150−600 cm^{-1} regions with 0.1% CO in neon are illustrated in Figures 1 and 2, respectively, and the absorptions are listed in Table 1. The stepwise annealing and photolysis behavior of these new product absorptions will be discussed below. Different isotopic carbon monoxides $^{13}C^{16}O$, $^{12}C^{18}O$ and $^{12}C^{16}O+^{13}C^{16}O$, $^{12}C^{16}O+^{12}C^{18}O$ mixtures were employed for product identification through isotopic shifts and splittings. The isotopic counterparts are also listed in Table 1. The mixed $^{12}C^{16}O+^{13}C^{16}O$ spectra in the 2060−1670 cm^{-1} and 900−580 cm^{-1} regions are shown in Figures 3 and 4, and the

(15) Zhou, M. F.; Andrews, L.; Li, J.; Bursten, B. E. *J. Am. Chem. Soc.* **1999**, *121*, 9712.
(16) A preliminary report of the CThO and ThCO molecules has been communicated, see: Zhou, M. F.; Andrews, L.; Li, J.; Bursten, B. E. *J. Am. Chem. Soc.* **1999**, *121*, 12188.
(17) Burkholder, T. R.; Andrews, L. *J. Chem. Phys.* **1991**, *95*, 8697.
(18) Hassanzadeh, P.; Andrews, L. *J. Phys. Chem.* **1992**, *96*, 9177.
(19) ADF 2.3, Theoretical Chemistry, Vrije Universiteit, Amsterdam: Baerends, E. J.; Ellis, D. E.; Ros, P. *Chem. Phys.* **1973**, *2*, 42. te Velde, G.; Baerends, E. J. *J. Comput. Phys.* **1992**, *99*, 94. Fonseca Guerra, C.; Visser, O.; Snijders, J. G.; te Velde, G.; Baerends, E. J. In *Methods and Techniques for Computational Chemistry*; Clementi, E., Corongiu, G., Eds.; STEF: Cagliari, 1995; p 305.
(20) (a) Slater, J. C. *Quantum Theory of Molecular and Solids*; McGraw-Hill: New York, 1974; Vol. 4. (b) Vosko, S. H.; Wilk, L.; Nusair, M. *Can. J. Phys.* **1980**, *58*, 1200.
(21) Perdew, J. P.; Wang, Y. *Phys. Rev. B* **1992**, *45*, 13244. (b) Perdew, J. P.; Chevary, J. A.; Vosko, S. H.; Jackson, K. A.; Pederson, M. R.; Singh, D. J.; Foilhais, C. *Phys. Rev. B* **1992**, *46*, 6671.
(22) Ziegler, T.; Baerends, E. J.; Snijders, J. G.; Ravenek, W. *J. Phys. Chem.* **1989**, *93*, 3050.
(23) Snijders, J. G.; Baerends, E. J.; Ros, P. *Mol. Phys.* **1979**, *38*, 1909.
(24) Li, J.; Bursten, B. E. In *Computational Organometallic Chemistry*; Cundari, T. R., Ed.; Marcel Dekker: New York, 2001; p 345.
(25) Emsley, J. *The Elements*; Clarendon Press: Oxford, 1997.
(26) Ziegler, T.; Rauk, A.; Baerends, E. J. *Theor. Chim. Acta* **1977**, *43*, 261.
(27) (a) Li, J.; Bursten, B. E. *J. Am. Chem. Soc.* **1997**, *119*, 9021. (b) Li, J.; Bursten, B. E. *J. Am. Chem. Soc.* **1998**, *120*, 11456.
(28) Thompson, W. E.; Jacox, M. E. *J. Chem. Phys.* **1991**, *95*, 735.

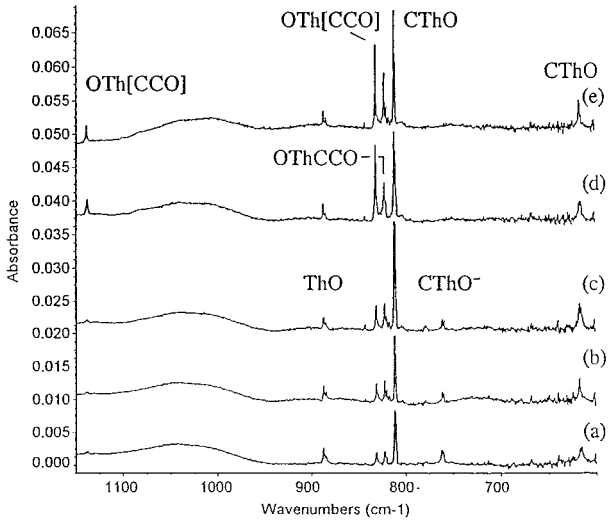

Figure 2. Infrared spectra in the 1150−600 cm^{-1} region for laser-ablated thorium co-deposited with 0.1% CO in neon at 4K: (a) after 30 min sample deposition, (b) after annealing to 8K, (c) after 15 min $\lambda > 470$ nm photolysis, (d) after 15 min full arc photolysis, and (e) after annealing to 10K.

mixed $^{12}C^{16}O+^{12}C^{18}O$ spectra in the 2060−1670 cm^{-1} and 900−710 cm^{-1} regions are illustrated in Figures 5 and 6, respectively. Figure 7 shows the spectra in the 1150−1100 cm^{-1} region for different isotopic CO samples after full-arc photolysis.

Discussion

The new reaction product absorptions will be identified according to isotopic substitutions as well as density functional theoretical calculations. Below we will separately discuss the experimental and theoretical results for these reaction products.

CThO. The matrix site-split doublets at 812.2, 811.0 cm^{-1} and 617.7, 617.0 cm^{-1} observed after sample deposition, greatly increased on $\lambda > 470$ nm photolysis. These two bands track together throughout all the experiments suggesting different modes of the same molecule. The 812.2, 811.0 cm^{-1} doublet shifted to 811.9, 810.6 cm^{-1} with $^{13}C^{16}O$ and to 769.2, 768.0 cm^{-1} with $^{12}C^{18}O$, giving a small 12/13 ratio (1.0004, 1.0005) and a large 16/18 ratio (1.0559, 1.0600). In contrast, the 617.7, 617.0 cm^{-1} doublet shifted to 595.0, 594.4 cm^{-1} with $^{13}C^{16}O$ and to 617.3, 616.7 cm^{-1} with $^{12}C^{18}O$, which define a large 12/13 ratio (1.0382, 1.0380) and a small 16/18 ratio (1.0006, 1.0005). The isotopic substitutions suggest that the upper doublet is mostly Th−O and the lower doublet mostly Th−C in vibrational character; consistent with these conclusions, the higher-energy stretching bands are much more intense than the lower-energy stretching bands because of the much larger change of the dipole-moment for the Th−O stretching mode. The mixed $^{12}C^{16}O+^{13}C^{16}O$ and $^{12}C^{16}O+^{12}C^{18}O$ isotopic spectra reveal only two isotopic bands and clearly indicate that only one O and one C atom are involved in these two modes. Analogous to the CUO molecule,[15] these two matrix site-split doublets are assigned to the Th−O and Th−C stretching vibrations of the CO-insertion product CThO.

The experimental Th−O stretching frequency of CThO is 74.9 cm^{-1} lower than that for ThO, observed at 887.1 cm^{-1} in solid neon,[29,30] which is consistent with its longer calculated Th−O distance.[31] Although there is no Th−C frequency available for comparison, the Th−C stretching frequency in CThO (617.7 cm^{-1}) is significantly lower than the U−C stretching frequency in CUO (1047.3 cm^{-1}), which seems to indicate that the Th−C bond in CThO is much weaker than the U−C bond in CUO. We will discuss the differences between CThO and CUO in detail later.

The present identification of CThO molecule is the first experimental discovery and characterization of this interesting triatomic molecule,[16] and its structure and bonding are anticipated to add to our understanding of small actinide-containing molecules. Inasmuch as the NThN molecule (isoelectronic to CThO) is linear[8] whereas OThO (isoelectronic to the linear uranyl ion UO_2^{2+}) and NThO are bent,[30,32,33] the determinations of the geometry and ground electronic state of CThO are of considerable interest. It is not apparent *a priori* whether CThO is linear or bent, and whether its ground state is a singlet or a triplet (or even higher spin multiplicity). To address these closely related questions, we have carried out linear transit (LT) calculations for the total energies of CThO vs the ∠C−Th−O angle (θ) for the singlet $(3a'')^2(8a')^2$ and triplet $(3a'')^2(8a')^1(9a')^1$ electron configurations (i.e. the $(3\pi)^4(6\sigma)^0$ and $(3\pi)^3(6\sigma)^1$ configurations of the linear structure) of the molecule. The results are presented in Figure 8. For both electron configurations, all the possible intermediate structures ($\theta = 30° - 180°$, step = 10°) have been fully optimized during the linear transit.

The LT surface for singlet CThO exhibits two local minima in the range $\theta = 0$ to 180°, one with an acute angle θ and one lying in a very flat energy surface near the linear structure.[34] The LT curve for the triplet state shows an overall lower energy than that of the singlet state, with a minimum for a strongly bent structure. Thus, we propose that the global minimum of CThO molecule corresponds to a bent structure with a triplet ground state. The optimized structure of CThO is shown in Figure 9(a). The optimized linear and bent geometries of CThO for the singlet, triplet, and quintet states are presented in Table 2. The lowest-energy singlet ($^1A'$) and quintet ($^5A''$) lie about 6.5 and 11.2 kcal/mol higher in energy than the triplet ($^3A'$) ground state. Interestingly, the linear structure is a transition state for the singlet, triplet, and quintet electronic states, as indicated by the imaginary vibrational frequencies (70*i*, 146*i*, and 102*i* cm^{-1}, respectively) for the C−Th−O bending modes. As is seen in Figure 8, the singlet potential energy surface near the linear structure is so flat that the strongly bent structure at $\theta = 148.5°$ is only lower in energy than the linear structure by a scant 0.1 kcal/mol! Although these results are calculated at the scalar relativistic level and there exists the possibility of singlet and triplet mixing due to spin−orbit coupling, we believe the ground state should be predominantly triplet in character due to the large singlet−triplet energy difference for the $(3a'')^2(8a')^1(9a')^1$ configuration.[35]

To compare the bonding in CThO to that in CUO, it is convenient to start with the molecular orbital diagrams of the

(29) Th + O_2 experiments were done in a neon matrix: ThO was observed at 887.1 cm^{-1}, ThO_2 at 756.8 (ν_3) and 808.4 cm^{-1} (ν_1); $Th^{18}O$ at 839.8 cm^{-1}, $Th^{18}O_2$ at 717.6 (ν_3) and 763.9 cm^{-1} (ν_1).

(30) Gablenick, S. D.; Reedy, G. T.; Chasanov, M. G. *J. Chem. Phys.* **1974**, *60*, 1167.

(31) Our calculations indicate that the ThO ($^1\Sigma^+$) molecule has Th−O = 1.853 Å which is 0.04 Å shorter than that in CThO (see Table 2). The IR frequency and intensity of ThO are calculated to be ν(Th−O) = 882 cm^{-1} and 175 km/mol, in good agreement with the experiment (see ref 29).

(32) Green, D. W.; Reedy, G. T. *J. Mol. Spectrosc.* **1979**, *74*, 423.

(33) (a) Kushto, G. P.; Andrews, L. *J. Chem. Phys.* **1999**, *103*, 4836. (b) Zhou, M. F.; Andrews, L. *J. Chem. Phys.* **1999**, *111*, 11044.

(34) Although we will not focus on the acute-angle structures that have the direct C−O bonding, we indeed find two structures for Th(η^2-CO), where the ∠C−Th−O angles for the singlet and triplet are 56.1° and 37.5°, respectively.

Table 1. Infrared Absorptions (cm^{-1}) from Codeposition of Laser-Ablated Th Atoms with CO in Excess Neon at 4K

$^{12}C^{16}O$	$^{13}C^{16}O$	$^{12}C^{18}O$	$^{12}C^{16}O+^{13}C^{16}O$	$^{12}C^{16}O+^{12}C^{18}O$	R(12/13)	R(16/18)	assignment
2048.6	1985.0	2028.0	2048.6, 2039.4, 1994.5, 1984.9	2048.5,2028.0	1.0320	1.0102	OThCCO
1999.7	1956.6	1951.2	1999.7, 1958.4	1999.8,1951.2	1.0220	1.0249	$Th(CO)_6$
1990.8	1948.2	1942.3	1990.9, 1947.9	1990.9, 1942.4	1.0219	1.0250	$Th(CO)_6$
1949.7	1907.7	1902.3			1.0220	1.0249	$Th(CO)_5$
1919.1	1876.4	1874.6	1918.9, 1907.6, 1894.0, 1876.4	1919.2, 1907.5, 1893.4, 1874.6	1.0228	1.0237	$Th(CO)_3$
1904.7	1863.7	1857.8			1.0220	1.0252	?
1897.3	1856.7	1850.7			1.0219	1.0252	$Th(CO)_4$
1882.2	1841.3	1836.9			1.0222	1.0247	?
1861.5	1821.4	1816.4			1.0220	1.0248	?
1827.7	1787.9	1784.2	1827.8, 1814.4, 1787.9	1827.8, 1813.8, 1784.2	1.0223	1.0244	$Th(CO)_2$
1817.5	1777.7	1774.3	1817.2,1777.4	1817.3,1774.8	1.0224	1.0243	ThCO
1810.8	1746.1	1799.3			1.0371	1.0064	OTh(η^3-CCO)
1809.1	1744.6	1797.0			1.0370	1.0067	OTh(η^3-CCO)
1803.6	1767.1	1760.3			1.0207	1.0246	$Th(CO)_3$
1775.6	1736.7	1733.8	1776.9, 1749.4, 1736.4	−1747.1, 1733.6	1.0224	1.0241	$Th(CO)_2$
1719.1	1682.2	1678.9	1718.9, 1705.3, 1681.8	1718.8, 1704.6, 1678.7	1.0219	1.0239	$Th(CO)_2$-OThCCO
1353.6	1317.0	1329.6					
1139.2	1114.2	1109.1	1139.1, 1128.9, 1125.2, 1114.3	1139.1, 1109.1	1.0224	1.0271	OTh(η^3-CCO)
1137.9	1113.0	1108.2	1138.1, 1127.8, 1123.9, 1113.2	1137.9, 1108.2	1.0224	1.0268	OTh(η^3-CCO)
887.1	887.1	839.9		887.1, 839.9		1.0562	ThO
884.5	884.5	837.4		884.5, 837.4		1.0562	ThO site
831.6	831.5	787.1		831.5, 787.2		1.0565	OTh(η^3-CCO)
822.5	822.5	778.9		822.4, 778.8		1.0560	OThCCO
812.2	811.9	769.2		812.2, 769.1	1.0004	1.0559	CThO
811.0	810.6	768.0		811.0, 768.0	1.0005	1.0600	CThO site
761.7	761.2	722.1		761.7, 722.1	1.0007	1.0548	$CThO^-$
759.6	759.3	720.3			1.0004	1.0546	$CThO^-$ site
617.7	595.0	617.3	617.7, 595.1		1.0382	1.0006	CThO
617.0	594.4	616.7	617.1, 594.5		1.0380	1.0005	CThO site

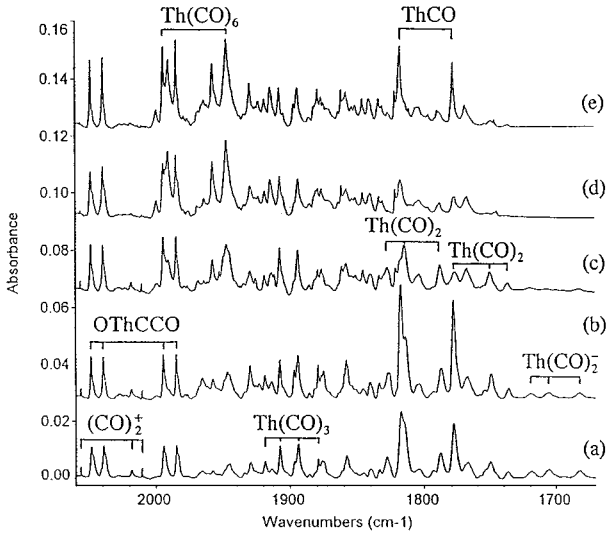

Figure 3. Infrared spectra in the 2060−1670 cm^{-1} region for laser-ablated thorium co-deposited with 0.1% $^{12}C^{16}O$ + 0.1% $^{13}C^{16}O$ in neon at 4K: (a) after 30 min sample deposition, (b) after annealing to 8K, (c) after 15 min λ > 470 nm photolysis, (d) after 15 min full arc photolysis, and (e) after annealing to 10K.

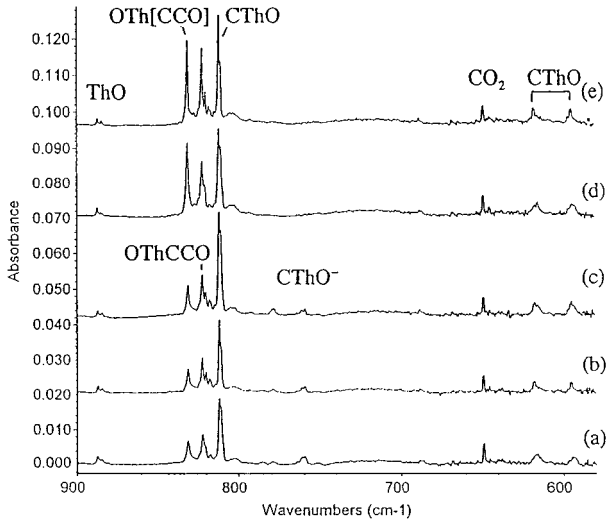

Figure 4. Infrared spectra in the 900−580 cm^{-1} region for laser-ablated thorium co-deposited with 0.1% $^{12}C^{16}O$ + 0.1% $^{13}C^{16}O$ in neon at 4K: (a) after 30 min sample deposition, (b) after annealing to 8K, (c) after 15 min λ > 470 nm photolysis, (d) after 15 min full arc photolysis, and (e) after annealing to 10K.

linear structures of the CAnO molecules, as illustrated in Figure 10. We can envision these molecules as being formed in two distinct steps that give an indication of the electronic charge flow that occurs: We first imagine lengthening the CO molecule, followed by insertion of the An atom into the CO bond. The CO molecule has the well-known ...$1\pi^4 5\sigma^2 2\pi^0 6\sigma^0$ frontier orbital configuration, where the 2π and 6σ MOs are strongly C−O antibonding. Lengthening the C−O bond decreases the degree of antibonding in these MOs, thus lowering their energy significantly. When the highly electropositive An atoms are inserted between the C and O atoms, the metal-based electrons lie at a higher energy than the CO 2π and 6σ MOs. As a consequence, the electrons are transferred from the metal to the largely C- and O-localized 2π and 6σ MOs of CAnO. In the case of CUO, all six valence electrons of the U atom are transferred, leading to the closed-shell...$1\pi^4 5\sigma^2 2\pi^4 6\sigma^2$ configuration and a $^1\Sigma^+$ ground state (in the $C_{\infty v}$ single group), which is analogous to the $^1\Sigma_g^+$ ground state of the isoelectronic UO_2^{2+} ion. This ground electronic configuration corresponds roughly to three U−O ($1\pi^4 5\sigma^2$) and three U−C ($2\pi^4 6\sigma^2$) bonds for the CUO molecule.

(35) Based on the calculated energy (−17.6915 eV) for the $(3a'')^2(8a'\uparrow)^1(9a'\downarrow)^1$ configuration, we have obtained the adiabatic singlet−triplet splitting energy as 9.3 kcal/mol using Ziegler's sum rule. For a discussion of singlet−triplet splitting energy calculations, see, for example, Hu, C.-H. *Chem. Phys. Lett.* **1999**, *309*, 81.

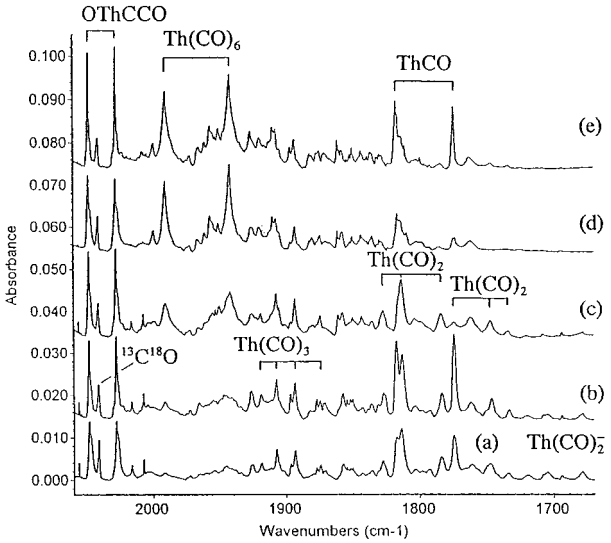

Figure 5. Infrared spectra in the 2060−1670 cm^{-1} region for laser-ablated thorium co-deposited with 0.1% $^{12}C^{16}O$ + 0.1% $^{12}C^{18}O$ in neon at 4K: (a) after 30 min sample deposition, (b) after annealing to 8K, (c) after 15min λ > 470 nm photolysis, (d) after 15min full arc photolysis, and (e) after annealing to 10K.

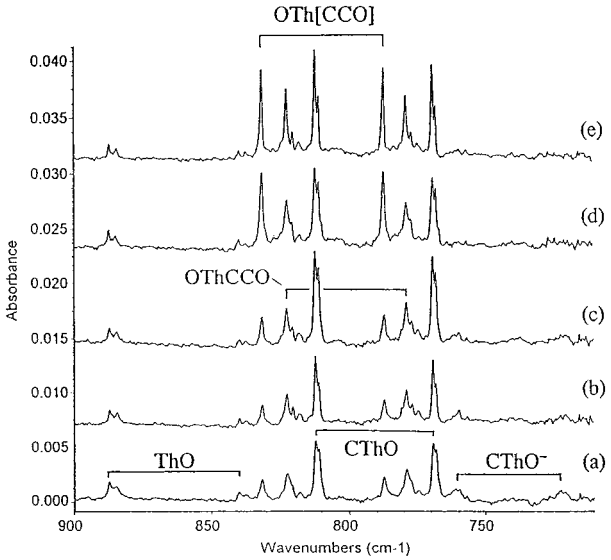

Figure 6. Infrared spectra in the 900−710 cm^{-1} region for laser-ablated thorium co-deposited with 0.1% $^{12}C^{16}O$ +0.1% $^{12}C^{18}O$ in neon at 4K: (a) after 30min sample deposition, (b) after annealing to 8K, (c) after 15min λ > 470 nm photolysis, (d) after 15min full arc photolysis, and (e) after annealing to 10K.

When a Th atom is inserted between the C and O atoms, the situation changes because Th has only four valence electrons. As a result, it is not possible to fill both the 2π and 6σ MOs of CThO simultaneously. As shown in Table 2, the DFT calculations predict that the lowest-energy state for linear CThO is the $^1\Sigma^+$ singlet from the $1\pi^4 5\sigma^2 2\pi^4 6\sigma^0$ configuration, corresponding to the transfer of all four Th electrons to the 2π MO of CThO and the formation of three Th−O ($1\pi^4 5\sigma^2$) and only *two* Th−C ($2\pi^4 6\sigma^0$) bonds. The low-lying $^3\Pi$ ($1\pi^4 5\sigma^2 2\pi^3 6\sigma^1$) and $^3\Sigma^-$ ($1\pi^4 5\sigma^2 2\pi^2 6\sigma^2$) triplet states, and the $^5\Sigma^-$ ($1\pi^4 5\sigma^2 2\pi^2 6\sigma^1 7\sigma^1$) quintet state of linear CThO lie 8.7, 12.5, and 9.7 kcal/mol higher in energy than the $^1\Sigma^+$ state, respectively.[36] As a result of the energetic closeness of the $^1\Sigma^+$ ($2\pi^4 6\sigma^0$) and $^3\Pi$ ($2\pi^3 6\sigma^1$) states in the linear geometry, the CThO molecule can easily undergo a symmetry-allowed bending distortion due to second-order Jahn−Teller instability (SOJT).[37]

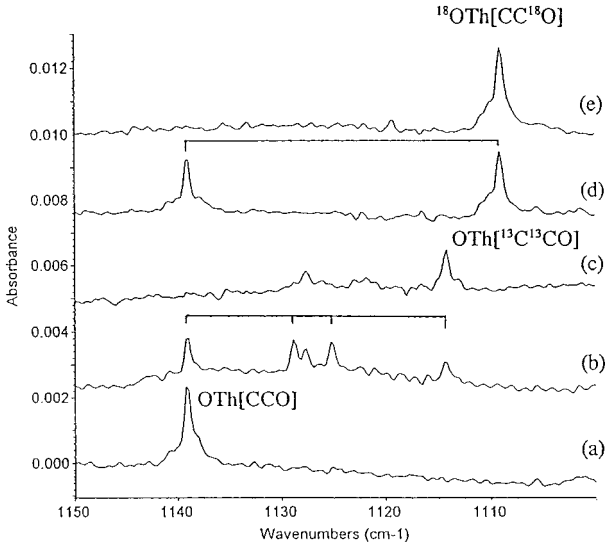

Figure 7. Infrared spectra in the 1150−1100 cm^{-1} region for laser-ablated thorium co-deposited with CO in neon at 4K after 15 min full arc photolysis: (a) 0.1% $^{12}C^{16}O$, (b) 0.1% $^{12}C^{16}O$ + 0.1% $^{13}C^{16}O$, (c) 0.1% $^{13}C^{16}O$, (d) 0.1% $^{12}C^{16}O$ + 0.1%$^{12}C^{18}O$, and (e) 0.1% $^{12}C^{18}O$.

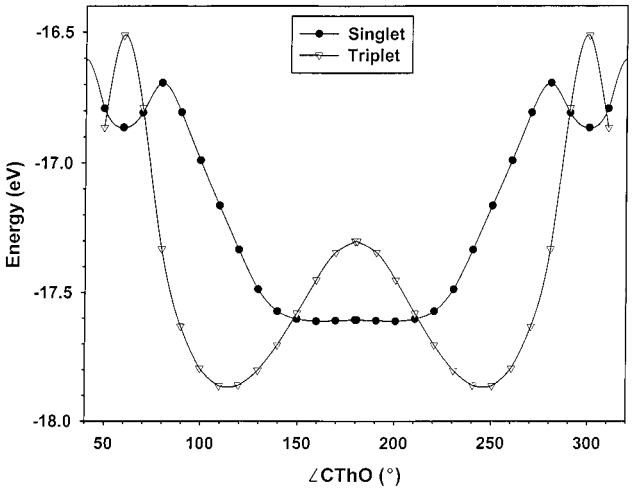

Figure 8. Linear transit energy curves for the singlet and triplet states of CThO.

A simple analysis of the bonding in CThO indicates that the overall bonding is stronger in the bent geometry. The 2π MO of C···O has the proper phase relationship to interact strongly with the Th 6dπ orbitals when Th is inserted between the C and O atoms. For linear CThO, however, the 6σ MO of C···O interacts predominantly with the np or nf orbitals of Th. If CThO is allowed to bend, the 9a′ MO of bent CThO, which originates from the 6σ MO of linear CThO, drops significantly in energy owing to the now-allowed interaction of the 6σ MO of C···O with the Th 6d orbitals. The stabilization of the 9a′ MO upon bending is great enough that bent CThO is predicted to have a ^{3}A′ ground state that corresponds to a $(3a'')^2(8a')^1(9a')^1$ electron configuration. This state, which is lower in energy than any of the states of linear CThO, correlates to the $^3\Pi$ ($2\pi^3 6\sigma^1$) state of linear CThO. As is evident in Figure 8, the degree of bending

(36) The Th 6s and 6p orbitals are retained in the valence space whereas the C and O 1s orbitals are frozen. Hence, the numbering of the electronic configurations of linear CThO has one more π-orbital than that of the CO ligand.

(37) For a discussion of the second-order Jahn−Teller effects, see, for example, Li, J.; Liu, C.-W.; Lu, J.-X. *J. Mol. Struct. (THEOCHEM)* **1993**, *280*, 223.

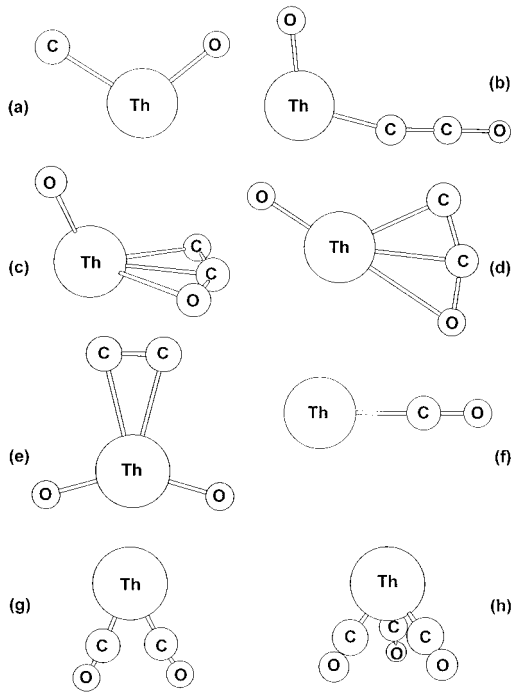

Figure 9. Optimized molecular structures of (a) CThO, (b) OThCCO, (c) OTh(η^3-CCO), (d) planar isomer of OTh(η^3-CCO), (e) (η^2-C_2)ThO_2, (f) ThCO, (g) $Th(CO)_2$, and (h) $Th(CO)_3$. The geometric parameters and vibrational frequencies of these molecules are given in Tables 2 and 3.

in CThO is quite significant inasmuch as the optimized C−Th−O bond angle is 108.9°.

The prediction of a bent triplet ground state for CThO is unusual but not unreasonable in light of a simple analysis of its valence electronic structure. The simplest Lewis structure for CThO is :C═Th═Ö:, which satisfies the tetravalency of Th but predicts that the molecule would be a carbene. Consistent with this notion, we find that the spin density of the $^3A'$ ground state of CThO resides predominantly (75%) on the C atom. Thus, CThO represents the first example of an actinide-containing carbene molecule. It is reminiscent of the well-studied organic carbene molecule ketenylidene (:C═C═Ö:), which also has a triplet ground state but has a linear structure.[38,39]

The correctness of this description of the ground state of CThO is corroborated by the calculated vibrational frequencies of CThO. The calculated vibrational frequencies for the optimized $^3A'$ ground state of $^{12}CTh^{16}O$ are 621 and 811 cm^{-1}, which compare remarkably well with the experimentally observed frequencies of 618 and 812 cm^{-1} (Table 1). The calculated infrared intensity ratio is 1:3.1, which is fairly close to the integrated band area ratio 1:3.8 observed in the experiment. An analysis of the normal modes shows that the 621 and 811 cm^{-1} vibrations correspond to the triatomic "symmetric" (in-phase) and "antisymmetric" (out-of-phase) bond stretching modes, respectively, although the former is predominantly a Th−C stretching mode whereas the latter is mainly a Th−O stretching mode. These conclusions are entirely consistent with the conclusions drawn from the experiments reported here with isotopically labeled CO.

To provide an additional comparison to the experimental results, we have also calculated the frequencies of $^{13}CTh^{16}O$ and $^{12}CTh^{18}O$, where ^{232}Th is assumed. The calculated 12/13 and 16/18 isotopic frequency ratios, 1.0383 and 1.0008 for the Th−C stretching and 1.0005 and 1.0558 for Th−O stretching, respectively, are in excellent agreement with the experimental ratios, thus further corroborating the experimental assignments. The calculated Mulliken overlap populations and the force constants indicate that the Th−C bond in CThO is much weaker than the U−C bond in CUO, which is in agreement with our previous experimental results as well.[15] It is also interesting to compare the stretching frequencies of XThO series (X = C, N, O). The vibrational frequencies of the "antisymmetric" Th−O stretch modes decrease whereas those of the "symmetric" modes increase from X = C to N to O, consistent with an increase in the X-Th bond order.[33]

$CThO^-$. The weak doublet at 761.7, 759.6 cm^{-1}, which is observed after deposition, decreases upon annealing, disappears after photolysis with $\lambda > 380$ nm, and fails to return upon further annealing. All of these observations suggest that the species formed is an anion. This doublet has a very small ^{13}C isotopic shift and large ^{18}O shift, which is reminiscent of the Th−O stretching mode of the CThO molecule, albeit at a frequency that is 50.5 cm^{-1} lower. No intermediate component was observed in the mixed isotopic experiments, so only one C and one O atom are involved in this mode. This doublet is assigned to the Th−O stretching vibration of the $CThO^-$ anion. The Th−C stretching vibration is not observed here, probably because its frequency is below the range we can measure.

As noted earlier, the ground state of neutral CThO has a bent structure with a $(3a'')^2(8a')^1(9a')^1$ electron configuration. Thus, if $CThO^-$ is also a bent species, its ground state might be a^2A' $(3a'')^2(8a')^2(9a')^1$, b^2A' $(3a'')^2(8a')^1(9a')^2$, or possibly higher spin-multiplicity states such as $^4A'$ $(3a'')^2(8a')^1(9a')^1(10a')^1$. Indeed, our DFT calculations predict a bent structure for $CThO^-$ (Table 2); all the states for linear structures lie higher in energy, with the lowest-energy $^2\Sigma^+$ state of $(3\pi)^4(6\sigma)^1$ configuration lying 11.1 kcal/mol higher than the a^2A' state of the bent structure. For the bent structure, the b^2A' state is found to be slightly higher in energy (4.1 kcal/mol) than the a^2A' state, whereas the $^4A'$ quartet state is only marginally (~0.17 kcal/mol) higher than the a^2A' state at the scalar relativistic level (Table 2).

The calculated vibrational frequencies of the various states of $CThO^-$ are also revealing with respect to identification of the species. For the a^2A' state, the Th−C and Th−O stretch frequencies are calculated to be 525 and 762 cm^{-1}, with the latter being much stronger (1:2.2) in intensities. In addition, the calculated 12/13 and 16/18 isotopic frequency ratios (1.0007 and 1.0552) for the Th−O stretching mode of the a^2A' agree extremely well with the experimental ratios, 1.0007 and 1.0548. The perfect agreement between the calculated Th−O frequency (762 cm^{-1}) and the experimental one (761.7 cm^{-1}) lends strong support to the experimental proposal about the formation of the $CThO^-$ anion. The predicted lower energy vibration is expected to be weak and is just outside the spectral range that we can sample effectively. For the $^4A'$ state, the predicted frequencies are 571 and 761 cm^{-1}; thus, the higher energy frequency is again in excellent agreement with the experimental observation. For this state, however, the lower energy band is predicted to be comparable in intensity with the higher energy band, and it is within our spectral range. The fact that this band is not observed leads us to propose the a^2A' ground state for $CThO^-$, with the $^4A'$ state slightly higher in energy. Because Th is less electronegative than C, it might be expected that the electron affinity of CThO is lower than that of CCO. Indeed, based on the calculated energies of the ground states of CThO and

(38) Devilliers, C.; Ramsay, D. A. *Can. J. Phys.* **1971**, *49*, 2839.
(39) Our PW91 DFT calculations shows that for ketenylidene the singlet states are less stable than the triplet, which has 61% spin-density on the terminal C atom.

Table 2. Geometries (Å, deg), Energies (eV), Vibrational Frequencies (cm^{-1}), and Infrared Intensities (km/mol) of CThO and $CThO^-$

state	configuration	Th−C	Th−O	C...O	θ	E (eV)	ν_1	ν_2	ν_3
				Linear CThO					
$^1\Sigma^+$	$(3\pi)^4(6\sigma)^0$	1.977	1.900	3.877	180	−17.6048	70i(−177)	753(2.1)	779(305)
$^3\Pi$	$(3\pi)^3(6\sigma)^1$	2.140	1.897	4.037	180	−17.2276	146i(−212)	571(104))	775(248)
$^3\Sigma^-$	$(3\pi)^2(6\sigma)^2$	2.440	1.875	4.319	180	−17.0606			
$^5\Sigma^-$	$(3\pi)^2(6\sigma)^1(7\sigma)^1$	2.414	1.877	4.291	180	−17.1821	102i(−20)	449(50)	827(248)
				Bent CThO					
$^1A'$	$(3a'')^2(8a')^2(9a')^0$	1.985	1.901	3.740	148.5	−17.6097	92(53)	742(24)	780(233)
$^3A'$	$(3a'')^2(8a')^1(9a')^1$	2.124	1.889	3.268	108.9	−17.8935	160(12)	621(57)	811(174)
a^3A'	$(3a'')^1(8a')^2(9a')^1$	2.172	1.892	3.527	120.3	−17.6389			
b^3A'	$(3a'')^1(8a')^1(9a')^2$	2.339	1.872	3.430	108.6	−17.2715			
$^5A'$	$(3a'')^1(8a')^1(9a')^1(10a')^1$	2.373	1.872	3.404	106.0	−17.4097	126(14)	468(54)	839(185)
				Linear $CThO^-$					
$^2\Sigma^+$	$(3\pi)^4(6\sigma)^1$	2.004	1.956	3.960	180	−18.6257	131i(−33)	679(146)	709(56)
$^2\Pi$	$(3\pi)^3(6\sigma)^2$	2.232	1.940	4.172	180	−18.3948			
$^4\Pi$	$(3\pi)^3(6\sigma)^1(7\sigma)^1$	2.214	1.942	4.156	180	−18.4683	158i(−31)	553(177)	724(342)
				Bent $CThO^-$					
a^2A'	$(3a'')^2(8a')^2(9a')^1$	2.199	1.924	3.318	107.0	−19.1134	159(12)	525(84)	762(188)
b^2A'	$(3a'')^2(8a')^1(9a')^2$	2.137	1.934	3.385	112.4	−18.9270			
$^4A'$	$(3a'')^2(8a')^1(9a')^1(10a')^1$	2.175	1.925	3.331	108.6	−19.1062	161(22)	571(135)	761(179)

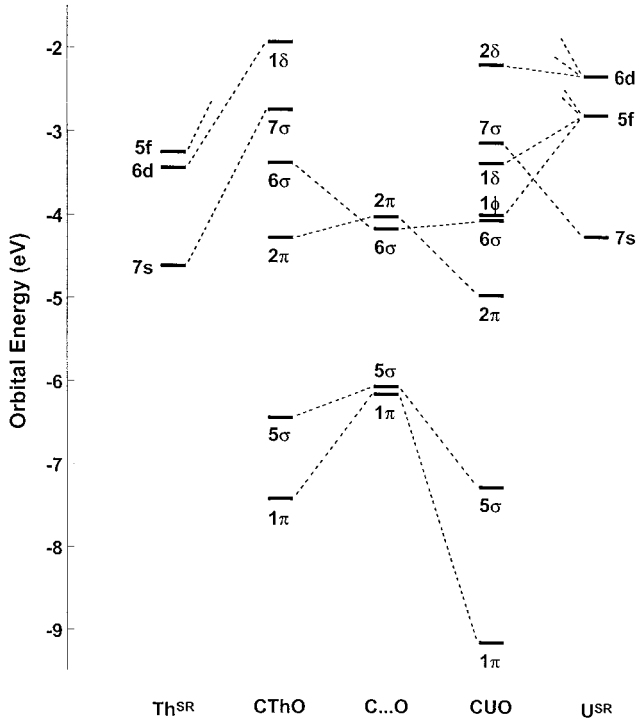

Figure 10. Comparison of the interactions of Th and U with a "separated" C···O molecule to form the molecular orbitals of CThO and CUO, respectively. The energy levels of Th^{SR} and U^{SR} are those for scalar relativistic atomic calculations on Th and U, respectively. The final electron configurations are $7s^26d^2$ (Th), $7s^25f^36d^1$ (U), $1\pi^45\sigma^2$ (CO), $1\pi^45\sigma^22\pi^46\sigma^0$ (CThO), and $1\pi^45\sigma^22\pi^46\sigma^2$ (CUO).

$CThO^-$, the calculated electron affinity of triplet CThO is 1.21 eV, which is significantly lower than the electron affinity (2.289 or 2.310 eV) of ketenylidene.[40,41] Nevertheless, the positive electron affinity of CThO is consistent with the formation of $CThO^-$ anion.

OThCCO. The 2048.6 and 822.5 cm^{-1} bands observed after sample deposition increased together on annealing and on $\lambda >$ 470 nm photolysis, but decreased slightly on full arc photolysis. The 2048.6 cm^{-1} band shifted to 1985.0 cm^{-1} with $^{13}C^{16}O$ and to 2028.0 cm^{-1} with $^{12}C^{18}O$, giving the 12/13 ratio 1.0320 and 16/18 ratio 1.0102. These ratios are significantly larger and smaller, respectively, than diatomic CO ratios, suggesting strong coupling with another C atom. In the mixed $^{12}C^{16}O+^{13}C^{16}O$ experiment, a quartet with approximately 1:1:1:1 relative intensities was produced, while in the mixed $^{12}C^{16}O+^{12}C^{18}O$ experiment, a doublet with pure isotopic counterparts was found. These observations confirm that two inequivalent C atoms and one O atom are involved in this vibrational mode. The associated 822.5 cm^{-1} band shows no carbon isotopic shift, but shifts to 778.9 cm^{-1} using $^{12}C^{18}O$ sample, giving the 16/18 ratio (1.0560) which is just under the diatomic Th−O ratio (1.0562) observed in solid neon. In the mixed $^{12}C^{16}O+^{12}C^{18}O$ experiment, only pure isotopic counterparts are present, indicating that only one O atom is involved in this mode. These two bands are assigned to the C−O and Th−O stretching vibrations of the OThCCO molecule, by analogy to the previously characterized OUCCO, ONbCCO, and OTaCCO molecules.[15,42] The weak band at 1353.6 cm^{-1}, with ^{13}C and ^{18}O isotopic frequencies at 1317.0 and 1329.6 cm^{-1}, is assigned to the C−CO stretching vibration. The experimental ratio of the band intensities of the 822.5, 1353.6, and 2048.6 cm^{-1} peaks is 5:1:92.

The OMCCO molecule, which can be visualized as formed by CMO + CO or OM + CCO, is one of the fascinating new species found for the MC_2O_2 isomers.[15] Table 3 summarizes the structures, energies, and vibrational properties of several stable isomers for ThC_2O_2. Unlike OUCCO, which is a linear molecule,[15] we find that OThCCO has a singlet ground state with a bent structure ($^1A'$: O−Th = 1.886 Å, Th−C = 2.159 Å, C−C = 1.297 Å, C−O = 1.186 Å, ∠OThC = 111.5°, ∠ThCC = 165.9°, ∠CCO = 178.8°), as shown in Figure 9(b). It is interesting to note that the Th−C bond length in OThCCO is much shorter than that in OThCO (2.488 Å),[43] indicating much stronger bonding interaction between OTh and CCO than that between OTh and CO. Indeed the Th−C Mulliken overlap population is about 90% larger for OThCCO than for OThCO.

The OThCCO molecule is predicted to have a closed-shell structure with a large HOMO−LUMO energy gap (1.49 eV), which is a likely indicator of stability. Indeed, the bent structure of OThCCO is found to be more stable than the linear one by 12.2 kcal/mol at the scalar relativistic level. When spin−orbit effects are included, the energy difference of these two structures becomes 12.3 kcal/mol, indicating the expected negligible effect that spin−orbit coupling has on the energetics of these closed-

(40) Zengin, V.; Persson, B. J.; Strong, K. M.; Continetti, R. E. *J. Chem. Phys.* **1996**, *105*, 9740.
(41) Choi, H.; Mordaunt, D. H.; Bise, R. T.; Tayler, T. R.; Neumark, D. M. *J. Chem. Phys.* **1998**, *108*, 4070.

Table 3. Energies (eV), Geometries (Å, deg), Selected Vibrational Frequencies, (cm^{-1}) and Infrared Intensities (km/mol) for Isomers of ThC_2O_2

	structure	state	E_{tot}	geometry	frequencies
OThCCO	linear	$^1\Sigma^+$	−37.0539	O−Th = 1.884, Th−C = 2.196, C−C = 1.296, C−O = 1.187	141i(−157), 604(53), 796(395), 1348(72)
	bent	$^1A'$	−37.5821	O−Th = 1.886, Th−C = 2.159, C−C = 1.297, C−O = 1.186, ∠OThC = 111.5, ∠ThCC = 165.9, ∠CCO = 178.7	606(36), 807(236), 1350(40), 2082(1672)
OTh(η^3-CCO)	planar	$^1A'$	−37.3893	O−Th = 1.884, Th−C = 2.289, 2.447, Th−O = 2.693, C−C = 1.280, C−O = 1.249, ∠OThO = 179.4, ∠CCO = 154.8, ∠CThC = 31.1, ∠CThO = 27.6	78i, 663, 827, 1196, 1869
	nonplanar	^1A	−37.5293	O−Th = 1.883, Th−C = 2.331, 2.390, Th−O = 2.456, C−C = 1.276, C−O = 1.273, ∠OThO = 113.1, ∠CCO = 149.4, ∠CThC = 31.3, ∠CThO = 30.4	463(151), 822(224), 1167(51), 1846(162)
(η^2-C_2)ThO_2	planar	$^3B_1$	−34.4998	Th−O = 1.934, Th−C = 2.621, C−C = 1.265, ∠OThO = 148.1, ∠CThC = 27.9, ∠OThC = 91.9, 119.9	327(68), 653(47), 689 (23), 1797(7)
	tetrahedral	$^3B_1$	−34.4723	Th−O = 1.934, Th−C = 2.683, C−C = 1.264, ∠OThO = 146.5, ∠CThC = 27.2, ∠OThC = 106.3	
$Th(CO)_2$	bent	a^1A_1	−34.4903	Th−C = 2.251, C−O = 1.188, C−C = 1.887, ∠CThC = 49.6, ∠ThCO = 175.6	410(62), 535(18), 1734(431), 1766(1314)
	bent	$^3B_1$	−34.3959	Th−C = 2.303, C−O = 1.176, C−C = 2.335, ∠CThC = 60.9, ∠ThCO = 174.0	
	bent	$^5B_1$	−34.3139	Th−C = 2.351, C−O = 1.171, C−C = 2.884, ∠CThC = 75.7, ∠ThCO = 176.5	
	bent	b^1A_1	−33.8010	Th−C = 2.291, C−O = 1.181, C−C = 3.871, ∠CThC = 115.3, ∠ThCO = 173.7	
	linear	$^1\Sigma^+$	−33.4532	Th−C = 2.333, C−O = 1.184	
	linear	$^3\Pi_g$	−33.7799	Th−C = 2.398, C−O = 1.171	
	linear	$^5\Pi_u$	−33.6340	Th−C = 2.426, C−O = 1.174	

shell molecules. This bent structure of OThCCO, which resembles that found for the analogous transition-metal complexes of ONbCCO (∠ONbC = 105.5°) and OTaCCO (∠OTaC = 103.5°),[42] can be attributed to the greater d-orbital participation in the bent form than in the linear form. The phenomenon that OThCCO prefers bent while OUCCO prefers linear is analogous to the observation that d-orbital bonding is the major driving force for the bent structures of MO_2 (M = transition metals) and ThO_2 *vis-á-vis* the linear structure of UO_2^{2+}.[44,45]

Our DFT calculations on OThCCO predict two strong infrared vibrational modes at 807 and 2082 cm^{-1}; these predicted frequencies deviate from the experimentally observed ones by only −1.6% and +1.9%, respectively. The normal-mode analysis indicates that the two strong peaks correspond to O−Th stretching and C−O stretching modes, as was deduced from the experiments. The calculations also find the C−C−O stretching mode at 1350 cm^{-1} (−0.3% relative to the experimental value) and its calculated intensity is only 2% of the C−O stretching mode, completely consistent with experiment. The calculated intensity ratio of these three peaks is 6:1:42, which is in good agreement with the experimental results. Moreover, the theoretical 12/13 and 16/18 isotopic frequency ratios for the calculated 807, 1350, and 2082 cm^{-1} bands are 1.0001 and 1.0566, 1.0272 and 1.0193, and 1.0328 and 1.0101, respectively, which are in excellent agreement with the experimental ratios. Our calculations on the linear structure indicate that it will have similar vibrational frequencies in the high-energy portion of the spectrum. However, the calculated doubly degenerate bending frequency for the linear structure is imaginary (141i cm^{-1}), indicating that the linear structure is a transition state.

OTh(η^3-CCO). The bands at 831.6, 1137.9, and 1809.1 cm^{-1} are produced on full-arc photolysis, mostly at the expense of OThCCO. All three bands sharpen on further annealing to 10K, with the 1137.9 and 1809.1 cm^{-1} bands shifting to 1139.2 and 1810.8 cm^{-1}. The 831.6 cm^{-1} band shows no carbon isotopic shift, but shifts to 787.1 cm^{-1} with $^{12}C^{18}O$. The 16/18 isotopic ratio 1.0565 indicates a terminal Th−O stretching vibration. In the mixed $^{12}C^{16}O$+$^{12}C^{18}O$ experiment, the observed doublet confirms that only one O atom is involved in this mode. The 1139.2 cm^{-1} band shifts to 1114.2 cm^{-1} with $^{13}C^{16}O$ and to 1109.1 cm^{-1} with $^{12}C^{18}O$, giving the 12/13 ratio 1.0224 and the 16/18 ratio 1.0271. Notice the 12/13 ratio is the same as the diatomic CO ratio, while the 16/18 ratio is significantly higher than the diatomic ratio. In the mixed $^{12}C^{16}O$+$^{13}C^{16}O$ experiment, a quartet with approximately 1:1:1:1 relative intensities was produced, while in the mixed $^{12}C^{16}O$+$^{12}C^{18}O$ experiment only pure isotopic counterparts were present, indicating that there are two slightly inequivalent C atoms and one O atom involved in this mode. The higher 16/18 ratio suggests that the O atom has antisymmetric vibrational character. The 1810.8 cm^{-1} band exhibited a large 12/13 ratio (1.0371) and a small 16/18 ratio (1.0064), which is characteristic of a predominantly C−C stretching vibration. These three bands are assigned to the Th−O, CC−O, and C−CO stretching vibrations of an exocyclic OTh[CCO] molecule.

Our DFT calculations find a ^1A ground state for OTh[CCO], which has a nonplanar structure with a bent O−Th−O angle (113.1°), as shown in Figure 9(c). This bent form, which has a remarkably large HOMO−LUMO energy gap (2.44 eV), is more stable by 3.2 kcal/mol than a similar planar structure with a linear ∠OThO angle [Figure 9(d)], and is only marginally less stable (1.2 kcal/mol) than the most stable noncyclic structure for OThCCO [Figure 9(b)]. When spin−orbit coupling effects are included, bent OTh[CCO] is 3.6 kcal/mol more stable than planar OTh[CCO] but 1.7 kcal/mol less stable than noncyclic OThCCO. The optimized bond lengths for the structure in Figure 9(c) are Th−O = 1.883, 2.456 Å and Th−C = 2.331, 2.389 Å. These distances indicate significant interactions between Th and all three atoms in the CCO group. The C−C−O group forms a plane with the Th atom in both the planar or nonplanar structure, and is slightly bent (∠C−C−O = 154.8° and 149.4°) to

(42) Zhou, M. F.; Andrews, L. *J. Phys. Chem.* A **1999**, *103*, 7785.
(43) Andrews, L.; Zhou, M. F.; Liang, B.; Li, J.; Bursten, B. E. *J. Am. Chem. Soc.* **2000**, *122*, 11440.
(44) (a) Tatsumi, K.; Hoffmann, R. *Inorg. Chem.* **1980**, *19*, 2656. (b) Wadt, W. R. *J. Am. Chem. Soc.* **1981**, *103*, 6053. (c) Pyykkö, P.; Lohr, L. L., Jr. *Inorg. Chem.* **1981**, *20*, 1850. (d) Pyykkö, P.; Jové, J. *New J. Chem.* **1991**, *15*, 717.
(45) Pepper, M.; Bursten, B. E. *Chem. Rev.* **1991**, *91*, 719.

accomplish better bonding with the Th atom. This molecule is thus best formulated as an O═Th unit coordinated to an η^3-CCO ligand, that is, as OTh(η^3-CCO).

The frequency calculations indicate that the planar OTh(η^3-CCO) is only a transition state with one imaginary frequency (78*i* cm^{-1}), whereas all of the frequencies of nonplanar OTh(η^3-CCO) are real, with the smallest frequency at 103 cm^{-1}. The calculated higher-energy frequencies are 822, 1167, and 1845 cm^{-1}, with a calculated intensity ratio of 4.3:1:3.1. The calculated 12/13 and 16/18 isotopic frequency ratios for these three modes are 1.0001 and 1.0566, 1.0197 and 1.0296, and 1.0381 and 1.0034, respectively. The normal-mode analysis shows that the three peaks are predominantly O−Th, CC−O, and C−CO stretching modes, respectively, as was concluded from the isotopic experiments. These calculated frequencies, intensities, normal modes, and isotopic frequency ratios are all in good agreement with the experimental observations, supporting the identification of this rare OTh(η^3-CCO) molecule. We also predict a CCO bending mode at 463 cm^{-1} with a predicted intensity comparable to that of the peak at 1845 cm^{-1}, but this region is not readily accessible experimentally.

It is worth noting that the structures of the OThCCO molecule and the bent/planar OTh(η^3-CCO) molecules are highly unusual because they contain the end-on and side-on coordination of OTh by ketenylidene (:C═C═O). Inasmuch as CCO not only has π-bonds but also is a diradical localized on the terminal-carbon, it can serve as both a side-on and an end-on ligand. The OThCCO and OTh(η^3-CCO) molecules, along with the previously characterized OUCCO,[15] are the first actinide-containing molecules with a CCO carbene as ligand. They are also, to our knowledge, the first examples of mononuclear ketenylidene complexes of any metal.[46]

(η^2-C_2)ThO_2. In our previous study of UC_2O_2 isomers, we identified a (η^2-C_2)UO_2 molecule with a distorted tetrahedral structure and C_2 point symmetry.[15] This molecule has a large HOMO−LUMO gap, implying that a stable electronic configuration has been reached. In fact, among the isomers of UC_2O_2, the stability increases as $U(CO)_2$ < OUCCO < (η^2-C_2)UO_2, i.e., the (η^2-C_2)UO_2 molecule is the most stable of the UC_2O_2 isomers. By extension, one might expect that a similar (η^2-C_2)ThO_2 molecule should be quite stable among the ThC_2O_2 isomers. At first glance, it may therefore be surprising that there is no evidence for the formation of (η^2-C_2)ThO_2 in the reactions of laser-ablated Th atoms with CO. Although (η^2-C_2)ThO_2 has not been identified experimentally, we can make use of theoretical methods to explore whether the absence of IR bands for the (η^2-C_2)ThO_2 molecule is due to its thermodynamic instability or perhaps because its IR intensities are too low to allow detection.

The absence of the (η^2-C_2)ThO_2 molecule in our experiments reminds us once again to consider one of the major differences between the two early actinide elements, U and Th. Our previous bonding analysis of the (η^2-C_2)UO_2 molecule revealed that its stability arises from the fact that (η^2-C_2)UO_2 could be viewed essentially as a complex in which a bent uranyl ion, UO_2^{2+}, is π-bonded to a closed-shell C_2^{2-} ligand, which is isoelectronic to the stable N_2 molecule. Thus, (η^2-C_2)UO_2 is viewed as an f^0 U(VI) complex. However, because a Th atom has two fewer valence electrons than a U atom, the stable closed-shell electron configuration of (η^2-C_2)UO_2 cannot be achieved by (η^2-C_2)ThO_2. The lowest energy geometry of (η^2-C_2)ThO_2 is the planar C_{2v} structure (Table 3). This molecule has a triplet ground state that corresponds to an ...$(8a_1)^1(5b_1)^1$ electron configuration. The two-half-filled orbitals are the two bonding MOs between the Th and the η^2-C_2 ligand, whereas in the case of (η^2-C_2)UO_2, both of these bonding orbitals are completely filled; thus, the metal-to-C_2 bonding is significantly weaker in the Th complex than in the U complex. Indeed, the Mulliken overlap population of Th−C in (η^2-C_2)ThO_2 is only about 25% of that of U−C in (η^2-C_2)UO_2. As a consequence, (η^2-C_2)ThO_2 is less stable than the OThCCO or OTh(η^3-CCO) isomers of ThC_2O_2. Nevertheless, our calculations predict that (η^2-C_2)ThO_2 is at least as stable as the experimentally identified $Th(CO)_2$ molecule (vide infra). Therefore, its absence in the IR spectra cannot be attributed to thermodynamic instability, but may be due to kinetic instability with respect to the other isomers, or the low IR intensities of the bands of the molecule, as we will now discuss.

As noted above, the lowest energy structure of (η^2-C_2)ThO_2 is the planar conformer with C_{2v} symmetry [Figure 9(e)], which is a different optimized geometry and point group than we found for (η^2-C_2)UO_2, which has C_2 symmetry. Optimization of the distorted-tetrahedral conformer of (η^2-C_2)ThO_2 (C_2 symmetry) leads to the same planar form, while the pseudo-tetrahedral conformer lies 0.6 kcal/mol higher in energy. As expected, the singlet states of the conformers of (η^2-C_2)ThO_2 all have higher energies than those of the triplet states. All of the (η^2-C_2)ThO_2 conformers lie ca. 70 kcal/mol higher in energy than the OTh(η^3-CCO) molecule (see Table 3). The OTh(η^3-CCO) structure can be considered as a distorted form of the (η^2-C_2)ThO_2 structure: The f^0 ThO_2 unit is unable to transfer metal-based electrons to the C_2 ligand, so the C_2 unit still remains some "free valence" and is therefore stabilized by bonding to the neighboring O atom. In this way, the seemingly unusual OTh(η^3-CCO) molecule achieves greater stability than (η^2-C_2)ThO_2.

The density functional calculations predict that all of the vibrational frequencies of the planar conformer of (η^2-C_2)ThO_2 are real, indicating that the structure is truly a minimum on the ThC_2O_2 potential surface (Table 3). Three of the vibrations are predicted in the experimentally accessible 400−3000 cm^{-1} range, namely the antisymmetric stretching (653 cm^{-1}) and symmetric stretching (689 cm^{-1}) modes of ThO_2 unit,[47] and the C═C stretching mode (1797 cm^{-1}) of the C_2 unit. These vibrational modes are analogous to those calculated at 849, 910, and 1755 cm^{-1} for the (η^2-C_2)UO_2 molecule.[15] The charge separation in (η^2-C_2)ThO_2 is smaller than that in (η^2-C_2)UO_2, so the dipole-moment derivatives and hence the IR intensities of the modes of (η^2-C_2)ThO_2 are reduced relative to those of (η^2-C_2)UO_2. The calculated IR intensities for (η^2-C_2)ThO_2 are only 47, 23, and 7 km/mol for the three vibrations (as compared to 79, 342, and 1 for (η^2-C_2)UO_2), which could make them difficult to be detected in the IR experiments.

$Th(CO)_n$ (n = 1−6). One of the most remarkable aspects of the present experiments is the production of the first binary carbonyl complexes of thorium, presumably from the direct reaction of Th atoms with CO in the noble gas host. We have previously communicated the production of the monocarbonyl complex, ThCO, which has a characteristic IR band at 1817.5 cm^{-1} for the $^{12}C^{16}O$ experiments.[16] This band is the strongest IR absorption immediately after sample deposition. It greatly

(46) See, for example: (a) Geoffroy, G. L.; Bassner, S. L. *Adv. Organomet. Chem.* **1988**, *28*, 1. (b) Calderazzo, F.; Englert, U.; Guarini, A.; Marchetti, F.; Pampaloni, G.; Segre, A.; Tripepi, G. *Chem. Eur. J.* **1996**, *2*, 412.

(47) Compared with the free ThO_2 molecule ($^1A_1$, PW91 geometry: O−Th = 1.911 Å, ∠OThO = 114.2°, frequencies: 157 (ν_b), 759 (ν_{as}), and 811 (ν_s) cm^{-1} with IR intensities of 26, 291, and 103 km/mol, cf. ref 29), the present asymmetric and symmetric stretching frequencies of ThO_2 unit are much lower, indicating the weakening of the Th−O bonding due to the coordination of the C_2 ligand.

increases on annealing, but decreases on $\lambda > 470$ nm photolysis when the IR bands for CThO greatly increase. The $^{13}C^{16}O$ and $^{12}C^{18}O$ counterparts at 1777.7 and 1774.3 cm^{-1} define 12/13 and 16/18 ratios of 1.0224 and 1.0243, respectively, which are characteristic of an essentially dinuclear C−O stretching mode. In the mixed $^{12}C^{16}O+^{13}C^{16}O$ and $^{12}C^{16}O+^{12}C^{18}O$ experiments, only pure isotopic counterparts were observed, which confirms the involvement of one CO submolecule. This band is assigned to the C−O stretching vibration of the ThCO molecule.

Our calculations predict that ThCO will have the linear structure shown in Figure 9(f) with Th−C = 2.261 Å and C−O = 1.181 Å. The state energy increases in the ordering of $^3\Sigma^-$ [$(6\sigma)^2(3\pi)^2$, 0.0 kcal/mol] < $^5\Delta$ [$(6\sigma)^1(3\pi)^2(1\delta)^1$, 3.2 kcal/mol] < $^3\Pi$ [$(6\sigma)^1(3\pi)^3$, 11.1 kcal/mol] ≪ $^1\Sigma^+$ [$(6\sigma)^0(3\pi)$,[4] 35.6 kcal/mol], i.e., the $^3\Sigma^-$ is the ground state.[48] This state lies only 2.4 kcal/mol higher in energy than the ground state of the CThO molecule. The predicted ground-state vibrational frequencies for the bending, Th−CO stretching, and C−O stretching modes are 292, 345, and 1790 cm^{-1}, respectively, with the latter being extremely intense (839 km/mol). The calculated CO-stretching frequency is only slightly lower (1.5%) than the observed 1817.5 cm^{-1} value, and the calculated 12/13 and 16/18 isotopic frequency ratios, 1.0229 and 1.0248, for C−O stretching vibration are in excellent agreement with the experimental values, once again providing strong corroboration for the experimental assignment.

ThCO is an unusual molecule in many respects. Its CO-stretching frequency is among the lowest of any neutral binary terminal metal carbonyl complex, which implies extensive metal-to-carbonyl back-bonding in this molecule. However, strong back-bonding is not generally associated with a non-closed-shell electronic structure. We believe that the unusual electronic structure of ThCO originates from a combination of the ground electron configuration and highly electropositive nature of the Th atom. ThCO is a Th(0) complex in which there are expected to be four predominantly Th-based electrons. The ground electron configuration of Th is $7s^26d^2$, i.e., the 5f orbitals are unoccupied in the ground-state atom. An MO diagram of the interaction of a CO ligand with a ground-state Th atom to form linear ThCO is presented in Figure 11, which also shows the expected stabilization of the 7s orbital and destabilization of the 5f and 6d orbitals due to relativistic effects.[49] Under $C_{\infty v}$ symmetry, the Th 6d orbitals correlate to the $3\pi + 1\delta + 8\sigma$ MOs, whereas the Th 5f orbitals correlate to the $4\pi + 1\phi + 7\sigma + 2\delta$ MOs. As usual, the dominant interactions are σ-donation from the filled CO 5σ MO and π-back-donation from the Th atom to the empty CO 2π orbitals. Because the 5f orbitals are much more radially contracted than the 6d orbitals, the orbital splitting due to CO coordination is much smaller for 5f orbitals (0.35 eV) than for the 6d orbitals (2.37 eV). Thus, as expected,[13] the CO-to-Th σ donation occurs mainly via the Th $6d\sigma$ orbital, an interaction that occurs in the 5σ MO of ThCO. The Th 7s and $5f\sigma$ orbitals are essentially unperturbed by this donation,

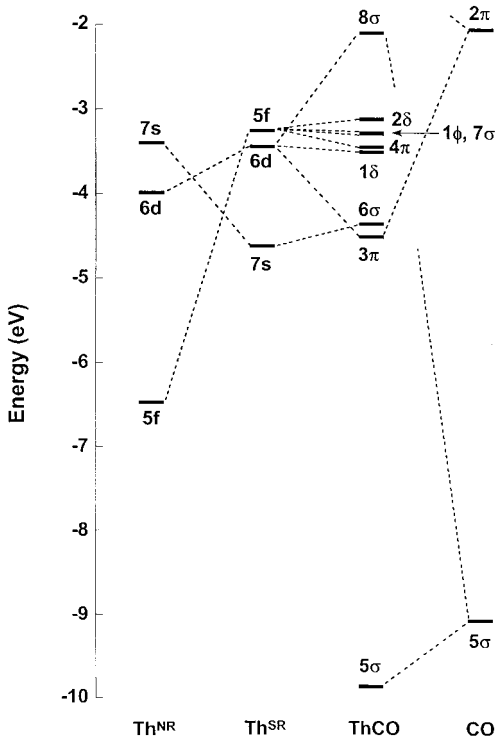

Figure 11. Energy level diagram showing the interaction of a CO ligand with a Th atom to form linear ThCO. The atomic energy levels of Th^{NR} and Th^{SR} are for nonrelativistic and scalar relativistic calculations on Th, respectively.

and thus the 6σ MO of ThCO is a nonbonding orbital that is largely Th 7s in character (83% Th 7s, 12% Th $6d_{z^2}$, 2% Th $5f_{z^3}$). The Th-to-CO π-back-bonding occurs via donation from the Th $6d\pi$ ($6d_{xz}$, $6d_{yz}$) orbitals, and leads to the doubly degenerate 3π MO (57% $6d\pi$ + 6% $5f\pi$ in ThCO vs 22% $6d\pi$ + 43% $5f\pi$ in UCO). Due to the high electronegativity of Th, this MO has a very large (36%) contribution from the CO ligand and thus represents a very strong back-bonding interaction. The relatively low energy of the Th 7s orbital causes the 6σ MO of ThCO to be nearly isoenergetic with the 3π MO, even though the former is largely nonbonding and the latter is strongly Th−CO π-bonding. As shown in Figure 11, the $^3\Sigma^-$ ground state corresponds to the $(6\sigma)^2(3\pi)^2$ electron configuration. It is remarkable that the CO stretching frequency in ThCO is reduced by >300 cm^{-1} relative to free CO despite only two of the Th-based electrons being involved in back-bonding. The highly electropositive nature of Th and the strong interaction between the diffuse Th $6d\pi$ orbitals and the CO 2π orbitals has led essentially to a one-electron reduction of the CO ligand.[50]

It is interesting to consider what the CO-stretching frequency of ThCO would be if all four Th-based electrons were involved in back-bonding. The $^1\Sigma^+$ excited state of ThCO, which lies ca. 36 kcal/mol above the ground state, corresponds to a $(6\sigma)^0(3\pi)^4$ electron configuration in which all four Th-based electrons are involved in Th−CO back-bonding. We have calculated the CO-stretching frequency of this excited state, and find it to be an astoundingly low 1630 cm^{-1}, a value considerably lower than the lowest known CO-stretching frequency of any terminal metal carbonyl.

Higher carbonyls are also evident in our experiments. Bands at 1827.7 and 1775.6 cm^{-1} are observed on deposition and

(48) As a comparison, parallel calculations of TiCO indicate that the ground state corresponds to $4s^13d^3$ configuration, where one 4s electron has been promoted due to CO coordination. We find that the ground state of TiCO is a quintet, in agreement with other recent DFT studies of the molecule: (a) Sosa, R. M.; Gardiol, P.; Beltrame, G. *Int. J. Quantum Chem.* **1998**, *69*, 371. (b) Zhou, M.; Andrews, L. *J. Phys. Chem. A* **1999**, *103*, 5259.

(49) For qualitative and quantitative discussions of direct and indirect relativistic effects, see, for example: (a) Pitzer, K. S. *Acc. Chem. Res.* **1979**, *12*, 271. (b) Pyykkö, P.; Desclaux, J.-P. *Acc. Chem. Res.* **1979**, *12*, 276. (c) Pyykkö, P. *Chem. Rev.* **1988**, *88*, 563. (d) Schwarz, W. H. E.; van Wezenbeek, E. M.; Baerends, E. J.; Snijder, J. G. *J. Phys.* **1989**, *B22*, 1515.

(50) See, for example: Görling, A.; Ackermann, L.; Lauber, J.; Knappe, P.; Rösch, N. *Surface Science* **1993**, *286*, 26.

increase together upon annealing. Both bands show carbonyl isotopic frequency ratios characteristic of a C−O stretch (Table 1). In both mixed isotopic experiments, triplets with approximately 1:2:1 relative intensities were observed for each band, indicating that two equivalent CO units are involved in these modes. The matching isotopic band asymmetries further verify that these two bands arise from a single molecule, and they are assigned to the symmetric and antisymmetric C−O stretching vibrations of the bent (C_{2v}) $Th(CO)_2$ molecule.

The $Th(CO)_2$ molecule represents another interesting member of the family of ThC_2O_2 isomers. There are three relatively low-lying states of the molecule, each of a different spin multiplicity in the absence of spin−orbit coupling. As shown in Table 3, the optimized geometries of the singlet (a^1A_1), triplet ($^3B_1$), and quintet ($^5B_1$) states of $Th(CO)_2$ all have strongly bent structures ($\angle$CThC = 49.6°, 60.9°, 75.7°, respectively). The a^1A_1 singlet is the ground state, and the structure of this state of the molecule is shown in Figure 9(g). Both the very acute $\angle$CThC angle and the singlet ground state of $Th(CO)_2$ are counterintuitive. We have therefore performed LT calculations for the singlet, triplet, and quintet states in order to determine with more certainty the minimum-energy geometry and electronic state. These calculations indicate that all the bent structures of the singlet, triplet, and quintet states lie significantly lower in energy than their linear counterparts, with the bent a^1A_1 singlet state being most stable. Singlet $Th(CO)_2$ molecule has two local minima above the ground state, one for a linear ($^1\Sigma^+$) and one for a moderately bent (b^1A_1, $\angle$CThC = 115.3°) structure. These minima lie 24.0 and 16.0 kcal/mol above that of the strongly bent a^1A_1 ground state, respectively. The LT calculations confirm that the singlet state has a lower minimum energy than either the triplet or the quintet states.

For the a^1A_1 ground state of $Th(CO)_2$, we predict that the antisymmetric (B_1) and symmetric (A_1) stretching vibrational modes of the two CO ligands have infrared absorptions at 1734 and 1766 cm^{-1}, respectively. The calculated 12/13 and 16/18 isotopic frequency ratios, 1.0231 and 1.0242 for the B_1 mode and 1.0229 and 1.0244 for the A_1 mode, agree well with the experimental ratios, 1.0222 and 1.0239 (B_1) and 1.0223 and 1.0244 (A_1). As expected for an acute $M(CO)_2$ molecule, the symmetric stretch is more intense, by roughly a factor of 3 according to our calculations. These calculated frequencies (−2.3% and −3.3% in error), isotopic frequency ratios, and intensities are in fair agreement with the experimental data, supporting the experimental identification of $Th(CO)_2$. As shown in Table 3, $Th(CO)_2$ is less stable than the OThCCO molecule by 71.3 kcal/mol. The energetic ordering of the various isomers of ThC_2O_2 is seen to be OThCCO < OTh(η^3-CCO) ≪ (η^2-C_2)-ThO_2 < $Th(CO)_2$.

In light of our above discussion of ThCO, it is of interest to discuss briefly the bonding in $Th(CO)_2$. As is the case for ThCO, the CO-stretching frequencies of $Th(CO)_2$ are unusually low; in fact, the mean experimental CO-stretching frequency for the dicarbonyl (1802 cm^{-1}) is lower than the frequency observed for ThCO (1817.5 cm^{-1}). Inasmuch as the description of ThCO led to the conclusion that two of the four Th-based electrons are involved in back-bonding, the mean CO-stretching frequency would indicate that all four Th-based electrons are involved in back-bonding to the two CO ligands in the a^1A_1 ground state of $Th(CO)_2$. Indeed, we find this to be the case. The four Th-based electrons doubly occupy two MOs, each of which is involved in extensive Th 6d → CO 2π back-bonding. The first of these is the $7a_1$ MO that involves donation from a Th 7s/$6d_{z^2-x^2}$ hybrid orbital into in-plane CO 2π orbitals, whereas the second is the $3b_2$ MO in which density is donated from the Th $6d_{yz}$ orbital to the out-of-plane CO 2π orbitals:

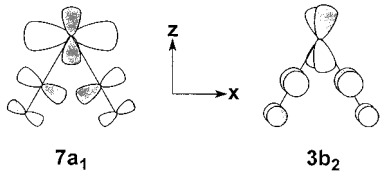

Owing to the electropositive nature of Th, both of these interactions achieve very strong back-donation into the CO ligands. The effectiveness of this donation is further increased by the acute $\angle$CThC angle: As is evident above, the carbon atoms of the CO ligands can be brought into close enough proximity to produce a significant C−C bonding interaction, which lowers the energies of the 2π group orbitals and facilitates even better Th-to-CO donation. The CO contributions to these back-bonding MOs are large enough to cause significant C−C bonding interactions, as is evident in the short C−C bond length of 1.887 Å. In essence, the strong Th 6d → CO 2π back-bonding has led to a three-center interaction and a partial reductive coupling of the two carbon atoms. The higher-spin excited states of $Th(CO)_2$, which involve depopulation of the C−C bonding orbitals depicted above, accordingly lead to longer C−C bond lengths (Table 3).

Evidence for the formation of $Th(CO)_3$ is provided by a sharp IR band at 1919.1 cm^{-1}. This feature was observed on deposition in higher CO concentration experiments, while in lower CO concentration experiments it was only observed on annealing. This band shifted to 1876.4 cm^{-1} with $^{13}C^{16}O$ and to 1874.6 cm^{-1} with $^{12}C^{18}O$, giving 12/13 ratio 1.0228 and 16/18 ratio 1.0237. In both mixed experiments, quartets with approximately 1:3:3:1 relative intensities were produced as shown in Figures 3 and 5. These quartet mixed isotopic structures are characteristic of the nondegenerate mode of a trigonal species. Accordingly, this band is assigned to the symmetric C−O stretching vibration of the $Th(CO)_3$ molecule under C_{3v} symmetry. A weaker broad band at 1803.6 cm^{-1} tracked with the 1919.1 cm^{-1} band, and is assigned to the doubly degenerate antisymmetric vibration of the $Th(CO)_3$ molecule.

The DFT calculations provide support for the C_{3v} structure for $Th(CO)_3$; all the optimizations of the low-symmetry geometries have higher energies or ultimately lead to the C_{3v} structure. The $Th(CO)_3$ molecule has a $^3A_2$ ground state and its optimized geometry parameters are Th−C = 2.308 Å, C−O = 1.172 Å, C−C = 2.588 Å, $\angle$CThC = 68.2°, $\angle$ThCO = 174.5°. Once again, the $Th(CO)_3$ molecule has a highly acute $\angle$CThC angle and strong C−C interaction. The higher vibrational frequencies in $Th(CO)_3$ relative to those of ThCO and $Th(CO)_2$ reflect the fact that maximum π-back-donation was achieved in the case of the dicarbonyl complex. The addition of another CO ligand requires that the back-bonding electron density be shared among a greater number of ligands, leading to higher IR frequencies. Our calculated frequencies for the symmetric C−O stretching mode and the double-degenerate modes are 1807 and 1885 cm^{-1}, respectively, which agree with the experimental values within 0.2% and −1.8%, respectively.

Several other bands in the high-energy portion of the IR spectrum increase upon annealing at the expense of the $Th(CO)_3$ absorptions, and we believe that these bands are due to higher binary carbonyl complexes. We tentatively assign the 1861.5 cm^{-1} band to $Th(CO)_4$, the 1949.7 cm^{-1} band to $Th(CO)_5$, and the 1990.8 cm^{-1} band to $Th(CO)_6$. We are presently

undertaking detailed theoretical investigations of these higher thorium carbonyl complexes.

$Th(CO)_2^-$. A weak broad band at 1719.1 cm^{-1} decreased on annealing and disappeared on photolysis. The isotopic 12/13 and 16/18 ratios are characteristic of carbonyl stretching vibrational ratios. In both mixed isotopic experiments, triplets with approximately 1:2:1 relative intensities were produced, indicating that two equivalent CO units are involved in this mode. This band is assigned to the symmetric C−O stretching vibration of the bent $Th(CO)_2^-$ anion. The antisymmetric stretching vibration is weaker and not observed here.

The electronic structure of the $Th(CO)_2^-$ anion follows naturally from our discussion of neutral $Th(CO)_2$. We would expect the additional electron to increase the overall degree of back-bonding, consistent with the lower IR frequency for the anion relative to the neutral. Our DFT calculations indicate that $Th(CO)_2^-$ has a $^2A_1$ ground state with the following geometric parameters: Th−C = 2.264 Å, C−O = 1.208 Å, C−C= 1.856 Å, ∠CThC = 48.4°, and ∠ThCO = 175.8°. The shorter C−C bond length in the anion indicates that the greater back-bonding has led to an increase in the C−C interaction. The calculated ∠CThC angle of $Th(CO)_2^-$ (48.4°) and $Th(CO)_2$ (49.6°) are the smallest ∠CMC angles found so far; significantly acute ∠CMC angles are also found for other dicarbonyl complexes of electropositive elements, including $U(CO)_2^-$ (61.6°), $U(CO)_2$ (76.2°),[15] $O_2U(CO)_2$ (65.1°), $O_2Th(CO)_2^-$ (72.1°),[43] $Nb(CO)_2$ (87.1°), and $Ta(CO)_2$ (87.3°).[42]

The calculated antisymmetric (B_1) and symmetric (A_1) CO-stretching frequencies of $Th(CO)_2^-$ are 1623 and 1660 cm^{-1}, respectively, with a calculated IR intensity ratio of 1:3.6. The calculated frequency of the symmetric stretch agrees reasonably well (−3.4%) with the measured data. Although the antisymmetric stretch is predicted to have a large intensity (469 km/mol), the experimental spectrum in this region is complicated by water absorptions.

Reaction Mechanisms

Laser-ablated thorium atoms co-deposited with CO molecules in excess neon produced thorium carbonyls as well as the CThO CO-insertion product. The bands for the thorium carbonyls increased on annealing, indicating that addition reactions (1) are exothermic and little or no activation energy is required. CThO is formed by reaction 2, which required some activation energy inasmuch as the CThO absorptions decreased on annealing and increased only on photolysis. The ThCO absorption disappeared on $\lambda > 470$ nm photolysis, which caused a 2× growth of CThO absorptions, suggesting that CThO is also produced via isomerization of the ThCO carbonyl, reaction 3.

$$Th + CO \rightarrow ThCO \quad (1a)$$

$$ThCO + CO \rightarrow Th(CO)_2 \xrightarrow{CO} Th(CO)_n \; (n = 3-6) \quad (1b)$$

$$Th^* + CO \rightarrow CThO \quad (2)$$

$$ThCO + h\nu \rightarrow CThO \quad (3)$$

The absorptions for OThCCO increased on annealing, during which those for CThO decreased, indicating that OThCCO can be formed by addition reaction 4. The absorptions for $Th(CO)_2$ decreased on $\lambda > 470$ and 380 nm photolysis and disappeared on $\lambda > 290$ nm photolysis. The absorptions for OThCCO increased on $\lambda > 470$ and 380 nm photolysis, but decreased on $\lambda > 290$ nm and full arc photolysis, during which the absorptions for $OTh(\eta^3\text{-CCO})$ greatly increased. These observations strongly suggest the successive photon-induced rearrangement of $Th(CO)_2$ to OThCCO and finally to $OTh(\eta^3\text{-CCO})$, reaction 5. Our DFT results in Table 3 indicate that these rearrangements are exothermic, but they probably require kinetic photoactivation.

$$CThO + CO \rightarrow OThCCO \quad (4)$$

$$Th(CO)_2 + h\nu \rightarrow OThCCO + h\nu \rightarrow OTh(\eta^3\text{-CCO}) \quad (5)$$

It is notable that in our experiments, we observed the rearrangement of OThCCO only to the $OTh(\eta^3\text{-CCO})$ molecule, with no evidence for the formation of $(\eta^2\text{-}C_2)ThO_2$ even though this molecule is somewhat lower in energy than $Th(CO)_2$ (Table 3). By contrast, the more electron-rich dicarbonyls $M(CO)_2$ (M = U, Nb, Ta), which also rearrange to form OMCCO, ultimately lead to the formation of the $(\eta^2\text{-}C_2)MO_2$ molecules.[15,42] It is not unreasonable to propose that the exocyclic complex $OM(\eta^3\text{-CCO})$ is the intermediate in the transformation of OMCCO to $(\eta^2\text{-}C_2)MO_2$. UO_2 has a triplet ground state, and TaO_2 and NbO_2 both have doublet ground states; thus, the complexation of MO_2 with C_2 is favored via charge transfer from the MO_2 unit to C_2. By comparison, ThO_2 has a closed-shell singlet ground state, so the electronically unsaturated $(\eta^2\text{-}C_2)ThO_2$ complex is less stable than the $OTh(\eta^3\text{-CCO})$ complex.

Finally, the $CThO^-$ and $Th(CO)_2^-$ anions are formed via electron capture by neutral molecules, reactions 6 and 7.

$$CThO + e^- \rightarrow CThO^- \quad (6)$$

$$Th(CO)_2 + e^- \rightarrow Th(CO)_2^- \quad (7)$$

Conclusions

The reaction of laser-ablated Th atoms with CO has produced two remarkable one-to-one adducts in ThCO and CThO as well as a series of interesting complexes such as OThCCO, $OTh(\eta^3\text{-CCO})$, and $Th(CO)_n$ ($n = 1-6$). The spectroscopic studies of these molecules in conjunction with relativistic DFT calculations underscore the fundamental differences between the chemistry of thorium and the analogous chemistry with uranium atoms. ThCO, which is the first thorium carbonyl complex, has a CO-stretching frequency that is ca. 100 cm^{-1} lower than that of UCO despite the fact that U has a greater number of valence electrons for back-bonding than does Th. The differences between ThCO and UCO are mainly reflective of the much more electropositive nature of thorium and its transition-metal-like electronic configuration, a difference that also leads to the unusual highly bent structure for $Th(CO)_2$. The insertion product CThO, which is predicted to be a bent triplet metallocarbene, is very different from CUO, which is a linear closed-shell molecule.[15] Once again, the very disparate behaviors of these two actinide carbide oxides can be attributed to the different valence electron configurations of the actinide atoms.

The differences between the chemistry of Th and U is further evidenced in this paper by the bent structure of OThCCO vs the linear structure for OUCCO, an observation that parallels the well-known difference in the geometries of the actinyls ThO_2 and UO_2^{2+}. The most dramatic difference in the chemistry of Th and U is demonstrated in the stability of the $(\eta^2\text{-}C_2)AnO_2$ molecules (An = Th, U). Whereas the stabilities of the UC_2O_2 isomers increase as $U(CO)_2 <$ OUCCO $\ll (\eta^2\text{-}C_2)UO_2$, those of the ThC_2O_2 isomers increase as $Th(CO)_2 < (\eta^2\text{-}C_2)ThO_2 \ll$

OTh(η^3-CCO) < OThCCO, the differences being reflective of the different number of valence electrons on the metal atom. These differences between seemingly parallel experiments highlight the potential for large variations in the chemistry of actinide-containing systems as the element of focus is changed. The excellent agreement between the calculated and measured vibrational frequencies and IR intensities underscores the power of a combined experimental and theoretical approach in exploring challenging chemical problems involving actinide elements.

Acknowledgment. We gratefully acknowledge support for this research from the National Science Foundation (Grant CHE 97-00116 to L.A.), from the Division of Chemical Sciences, U.S. Department of Energy (Grant DE-FG02-86ER13529 to B.E.B.), from Los Alamos National Laboratory, and from the Ohio Supercomputer Center and the Environmental Molecular Sciences Laboratory at Pacific Northwest National Laboratory for grants of computer time.

IC010755M